Synthesis and Characterization of Novel Soybean-Oil-Based Elastomers with Favorable Processability and Tunable Properties

ARTICLE *in* MACROMOLECULES · NOVEMBER 2012

Impact Factor: 5.8 · DOI: 10.1021/ma301938a

8 AUTHORS, INCLUDING:

Jun MA
University of South Australia
97 PUBLICATIONS **1,850** CITATIONS
SEE PROFILE

Liqun Zhang
125 PUBLICATIONS **1,925** CITATIONS
SEE PROFILE

Hao Wang
JPS Health Network
90 PUBLICATIONS **675** CITATIONS
SEE PROFILE

Macromolecules

Article

pubs.acs.org/Macromolecules

Synthesis and Characterization of Novel Soybean-Oil-Based Elastomers with Favorable Processability and Tunable Properties

Zhao Wang,[†] Xing Zhang,[†] Runguo Wang,[†] Hailan Kang,[†] Bo Qiao,[†] Jun Ma,[§] Liqun Zhang,*[,†,‡] and Hao Wang[⊥]

[†]State Key Laboratory of Organic−Inorganic Composites, Beijing University of Chemical Technology, Beijing 100029, P R China

[‡]Key Laboratory of Beijing City on Preparation and Processing of Novel Polymer Materials, Beijing University of Chemical Technology, Beijing 100029, P R China

[§]School of Advanced Manufacturing and Mechanical Engineering, University of South Australia, SA5095, Australia

[⊥]Centre of Excellence in Engineered Fibre Composites and Faculty of Engineering, University of Southern Queensland, Qld 4350, Australia

Supporting Information

ABSTRACT: A new series of soybean-oil-based elastomers poly(epoxidized soybean oil-*co*-decamethylene diamine) (PESD) was synthesized by ring-opening polymerization from epoxidized soybean oil (ESO) and decamethylene diamine (DDA) in different molar ratios. The effect of the molar ratio on the structure and properties of PESD was identified by various methods. According to the results of Fourier transform infrared spectroscopy (FTIR), nuclear magnetic resonance (^{1}H NMR) and thermogravimetry (TGA), the glycerol center of ESO was broken by ammonolysis as expected in the process of polymerization, which resulted in un-cross-linked elastomers with low glass transition temperatures (T_g) ranging from −30 to −17 °C. PESD-3 (molar ratio of DDA to ESO is 2:1) was found to have the highest molecular weight and was most suitable for further processing. Then, PESD-3 was successfully cross-linked through succinic anhydride by a general rubber processing method to obtain a cross-linked bioelastomer. The mechanism of chain growth, ammonolysis of ester group, and cross-linking of PESD-3 was studied. The tensile strength of cross-linked PESD could be flexibly adjusted from 0.8 to 8.5 MPa by using different amounts of succinic anhydride without reinforcing fillers. The final bioelastomer possesses good damping property, low water absorption, and low degradation rate in phosphate buffer solution. These properties indicate potential engineering applications.

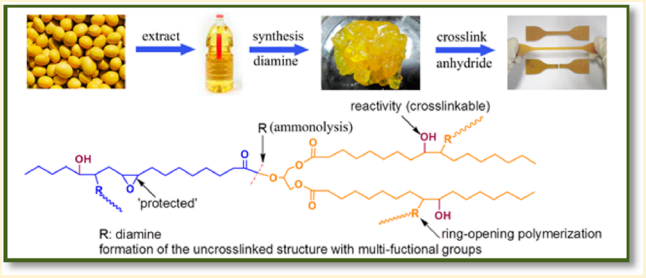

1. INTRODUCTION

Elastomer plays a very important role in our daily life. However, most synthetic elastomers are petroleum-based. To meet the growing demand for sustainable development, it is imperative to explore renewable raw materials to synthesize biobased elastomers as next-generation rubbers. Renewable natural resources, including lignin, carbohydrates, starch, proteins, and plant oil, have attracted increasing interests because of their low cost, large production, nontoxicity, ready availability.[1,2] Compared with other natural materials, plant oil has a relatively high reactivity to be used as a monomer for polymerization directly.[3−14] Soybean oil (SO), a major plant oil containing more than 99% of triglycerides, has been used since the early nineties in many products like soaps, paints, coatings, lubricants, and bioplastics.[15,16]

SO contains 23.4% of oleic, 53.3% of linoleic, 7.8% linolenic, and around 15% of palmitic and stearic acids,[5] in which the major unsaturated chains lead to cross-linked products. A low-cross-linked product with weak mechanical properties is obtained by using the cationic polymerization method because of the small amount and low reactivity of the internal double bonds of SO. Larock et al. produced low-saturation soybean oil and conjugated soybean oil by modifying SO, and then synthesized highly cross-linked thermosetting plastics with some aromatic comonomers by the free-radical method.[17,18] The high cross-link density and rigid structure conduced to good mechanical properties, but resulted in high glass transition temperature (T_g) which is not appropriate for preparing elastomers. Larock et al. also synthesized thermosetting elastomers[19,20] by using Norway fish oil (NFO) modified boron trifluoride diethyl etherate as catalyst. Epoxidized soybean oil (ESO), which is easily obtained from SO, was brought forward to synthesize polymers by using its epoxy groups.[21−27] Since the epoxy ring can be opened by amine or acid, ESO was used to react with polyamine, polyacid, or anhydride to form polymers.[28−31] In addition, polyols and

Received: September 15, 2012
Revised: October 29, 2012
Published: November 5, 2012

carbonated soybean oil (CSO) were used as monomers to synthesize polyurethane with different reactants.[32−36]

Up to now, almost all these methods preferably produce thermosetting polymers, which are not suitable for further processing. However, secondary processing may improve the material properties. In rubber industry, common raw rubbers are generally mechanically mixed with various ingredients to obtain good mechanical performance or special properties. Therefore, it is interesting and meaningful to synthesize processable elastomers from soybean oil. In our previous studies, biobased elastomers[37,38] that are both processable and cross-linkable were designed and synthesized, exhibiting good comprehensive properties. In addition, we were the first to prepare biobased engineering elastomers, which are different from degradable elastomers.[39−44]

In this study, a class of soybean-oil-based, processable and cross-linkable elastomers poly(epoxidized soybean oil-*co*-decamethylene diamine) (PESDs) was first designed and synthesized. ESO was employed to react with a diamine by combining the ring-opening reaction with ammonolysis, in which the ring-opening reaction contributes to chain growth and the ammonolysis is expected to break the glycerol center. Decamethylene diamine (DDA), a major raw material for synthesizing Nylon-1010, was chosen because it is a biomass that can be derived from castor oil.[45] In addition, the long carbon chain of DDA preferably forms a polymer with low T_g, which is a necessary condition for elastomer. Then one PESD was cross-linked by utilizing succinic anhydride as cross-linker according to a conventional rubber processing procedure. Succinic anhydride, a biomass that can be produced through the fermentation of glucose,[46,47] was selected because it can not only react with the amine group, epoxy group, or hydroxyl group of PESD to form a cross-linked structure, but also reduce water while reacting with the hydroxyl group. Finally, the cross-linked bioelastomer with tunable properties and practical significance was successfully prepared.

2. EXPERIMENTAL SECTION

2.1. Materials. ESO (epoxy value 6.5) has no double bond left, since all double bonds turned into epoxy groups. Epoxy value refers to an oxygen content of epoxy ethyl in 100g sample. ESO, a gift from Guangzhou Dongfeng Chemical Industrial Co., Ltd. (China), was dried in a vacuum oven at 80 °C for 6 h. Decamethylene diamine (purity >98%), which can be obtained from castor oil, was purchased from HWRK Chemical Inc. (China) and was purified by recrystallization for three times. Dibutylamine and succinic anhydride (>99.8%) were obtained from Aldrich Chemical Inc. (USA).

2.2. Synthesis of PESD with ESO and DDA. The ring-opening reaction of ESO and DDA was carried out in a 100 mL four-mouth flask equipped with a thermometer and a spherical condenser. DDA and ESO in given molar ratios (1.5:1, 1.75:1, 2:1, 2.25:1, and 2.5:1) were added into the flask, which was sealed and vacuumized to −0.1 Pa for 10 min. The system was then purged with high purity nitrogen, stirred at 250 rpm, and heated to 130 °C. The reaction was terminated after 6−10 h, depending on when the product started to climb onto the stirring paddle. The products with molar ratios of DDA to ESO of 1.5:1, 1.75:1, 2:1, 2.25:1, and 2.5:1 were named PESD-1, PESD-2, PESD-3, PESD-4, and PESD-5 respectively. The molecular weight of the biopolymer could not be obtained by GPC because the −NH functional group was absorbed by the chromatographic column.

Dibutylamine, the −NH of which is more active than the generated −NH from the ring-opening reaction, was first used to study the reaction of −NH with the epoxy ring. Under the same conditions as those used for the reaction between DDA and ESO, dibutylamine was found not to react with ESO, according to the FTIR spectra (see Supporting Information, Figure S1). Thus, the generated −NH would not react with the epoxy ring to form a cross-linked structure.

2.3. Soxhlet Extraction. A 1-g sample of each PESD was extracted for 36 h with 300 mL of refluxing tetrahydrofuran in a Soxhlet extractor. After extraction, the resulting solution was concentrated by rotary evaporation. Then the soluble fraction and insoluble fraction were dried in a vacuum oven at 60 °C, and the insoluble solids were weighed.

2.4. Cross-Linking of PESD-3. The cross-linking procedure of PESD-3 was similar to that of conventional rubber (such as natural rubber, styrene−butadiene rubber, ethylene propylene diene monomer rubber, et.al.). 50 g of PESD-3 was put into a two-roll mill (Φ160 mm) the distance of which was adjusted to the smallest gap. A given amount of the cross-linker succinic anhydride (3 phr, 5 phr, 7 phr, 9 phr, or 11 phr, phr stands for one gram per a hundred gram of elastomer) was then added in several installments. The final compound was then vulcanized in a compression molding press under a pressure of 10 MPa. The cross-linked PESD-3 is called bioelastomer in this paper.

2.5. Methods. FTIR spectra of the samples were recorded on a TENSOR27 (Bruker Optic GMBH, Germany) Fourier transform infrared spectrophotometer equipped with a Smart Orbit diamond attenuated total reflection (ATR) accessory. Absorption spectra were acquired at 4 cm^{-1} resolution and the signal averaged over 32 scans. Interferograms were Fourier transformed by using cosine apodization for optimum linear response. All spectra were baseline corrected and normalized to the average of the methyl peaks at 1463 cm^{-1}. ^1H NMR spectra were recorded by using a Bruker AV400 NMR spectrometer (Bruker, Germany) at a frequency of 400 MHz with $CDCl_3$ as solvent. The unchanged integral of CH_3 was selected as the primary integral 1 to all the PESD samples. The molecular weights of PESDs were determined by Multiangle static laser light scattering method on a DAWN HELEOS 114-H instrument (Wyatt Technology Corporation, USA) using tetrahydrofuran (THF) as the solvent. DSC thermograms of the samples were recorded by using a STARe system DSC1 Instruments (Mettler-Toledo International Inc., Switzerland). The samples in the form of small rectangles about 0.2 mm thick were accurately weighed and sealed in aluminum crucibles. The temperature was first raised to 100 °C at 10 °C per minute, allowed to stay there for 5 min to eliminate any thermal history and moisture from the sample, and then lowered to −100 °C at 10 °C per minute. Data were recorded in the temperature range −100 to +100 °C at a heating rate of 10 °C per minute. The nitrogen flow was 150 mL per minute. The measurements of sample weight loss were carried out on a STARe system TGA/DSC1 thermogravimeter (Mettler-Toledo International Inc., Switzerland) with a cooling water circulator. The testing was done under a flowing nitrogen atmosphere (20 mL/min). All the samples used in the thermogravimetric measurements were similar in weight (10 ± 1 mg) and heated from 30 to 800 °C at a heating rate of 10 °C/min. The cross-linking dynamics was determined by a P 3555 B 2 rotor vulcameter (Beijing Huanfeng Chemical Machinery Experimental Factory, China). About 7 g of PESD was vulcanized at 180 °C. The mechanical properties of all vulcanizates were measured at 25 °C according to ASTM D638 with a CMT4104 electronic tensile tester (SANS, China) at a crosshead speed of 500 mm/min. The dumbbell-shaped samples (25 mm × 6 mm × 2 mm) were prepared according to ISO/DIS 37−1990. The Mooney viscosity was measured by a M3810C Mooney viscometer (Beijing Huanfeng Chemical Machinery Experimental Factory, China) at 100 °C. Dynamic mechanical measurements were carried out on a dynamic mechanical analyzer (DMAVA3000, 01 dB Co., Ltd., France). The specimens were 15 mm long, 15 mm wide and about 2 mm thick. The temperature dependence of the loss factor tan δ was measured in the range −50 to 120 °C at a frequency of 1 Hz and a heating rate of 3 °C/min. Contact angles were measured on an OCA15EC machine (Data-Physics, Germany) at ambient temperature. The water drops were dropped carefully onto the samples. The average value of five measurements performed at different positions on the same sample was taken as the contact angle.

The water absorption of the samples was characterized according to Chinese Standard GB/T 1034−2008. The specimens 10 mm long, 8

Table 1. Several Basic Parameters of PESDs

sample	PESD-1	PESD-2	PESD-3	PESD-4	PESD-5
molar ratio DDA:ESO	1.5:1	1.75:1	2:1	2.25:1	2.5:1
reaction time (h)	10	8	6	8	10
molecular weight ($M_w \times 10^{-4}$ /g/mol)	2.15 ± 0.34	3.86 ± 0.52	13.31 ± 0.64	6.15 ± 0.46	4.78 ± 0.42
gel content (wt %)	1	15	6	5	3

mm wide, and about 2 mm thickness were immersed in 200 mL of deionized water at room temperature. The weight gain was measured as a function of immersion time (24, 48, 98, 192, 384, and 576 h). The swelling degree was calculated by using the following equation:

$$\text{water absorption } (\%) = (W_t - W_0)/W_0 \times 100 \quad (1)$$

where W_t is the wet weight and W_0 is the original weight of the sample.

In vitro degradation was determined by eq 2. Rectangular specimens (approximately 2 mm thick) were placed in a small bottle containing 20 mL of phosphate buffer solution (PBS, pH 7.4) at 37 °C. Then the specimens were dried in a vacuum oven at 60 °C. The weight loss at time t was calculated according to eq 2:

$$\text{weight loss } (\%) = (W_{tt} - W_{00})/W_{00} \times 100 \quad (2)$$

where W_{00} is the initial mass and W_{tt} is the mass at tim t. Three replicate measurements were performed for the degradation test, and the average value was taken.

3. RESULTS AND DISCUSSION

3.1. Synthesis of Poly(epoxidized soybean oil-*co*-decamethylene diamine) (PESDs) with Favorable Processability. To the best of our knowledge, thermosetting soybean-oil-based polymers were inclined to form because of the special molecular structure of SO. As discussed in the introduction, the synthesis of a processable and cross-linkable elastomer was preferred, which could make a great progress in soybean-oil-based elastomers. To meet this objective, we need to break the glycerol center of ESO during the polymerization. In this study, DDA was used to react with epoxy groups to contribute to chain growth and with ester groups to break the glycerol center. Finally, a class of processable PESDs was successfully synthesized from ESO and DDA at 130 °C within 6−12h. Different molar ratios of DDA to ESO were considered (1.5:1, 1.75:1, 2:1, 2.25:1, and 2.5:1) in order to study the effect of the molar ratio of DDA to ESO on the structure and properties of PESD. All PESD were soft and rubbery, light yellow in color, and soluble in either ethanol or tetrahydrofuran. The temperature of 130 °C was found to be optimum because lower temperatures would result in very long reaction times (longer than 15 h) and higher temperatures would lead to the loss of DDA. The reaction was terminated when the product began to climb the stirrer shaft, in a phenomenon called the "Weissenberg effect". Extending the reaction time would not lead to further reaction because of the high viscosity of the sample, but might increase the gel content. In this study, PESD with high molecular weight and low gel content is preferred. Table 1 lists the weight-average molecular weights (M_w) and gel contents of PESDs with different molar ratios of DDA to ESO. With increasing molar ratio of DDA to ESO, the gel content of PESDs first increase and then decreases. This result suggests that low molar ratios of DDA to ESO favor the reaction between epoxy groups and amine resulting in the chain growth and ultimately a cross-link structure, while ammonolysis does not easily occur to break the initial cross-linking structure (the glycerol center). With higher molar ratio of DDA to ESO, more ester groups of the glycerol center take part in ammonolysis, which result in low gel contents. In fact, as long as one ester group of each glycerol center is broken, the initial cross-link structure will be destroyed. Therefore, the gel contents of PESD-3, PESD-4, and PESD-5 do not change significantly. The weight-average molecular weight (M_w) of PESDs is also affected by the molar ratio. PESD-1 and PESD-2 have low molecular weights, probably because of incomplete reaction between DDA and the epoxy groups, while PESD-4 and PESD-5 have low molecular weights as a result of ammonolysis. Thus, PESD-3 has the highest M_w (M_w = 13.31 ± 0.64 g/mol). FTIR and ^{1}H NMR spectroscopy were used to verify our assumption and to determine the structure of PESDs.

Figure 1 presents the FTIR spectra of the PESDs. With the increase in the molar ratio of DDA to ESO, the intensity of O−H stretching vibration at 3306 cm^{-1} increases and the intensity of epoxy group at 832 cm^{-1} decreases. These features indicate that the reaction between the epoxy groups and amine groups indeed occurred and the degree of reaction increased with the increase in molar ratio of DDA to ESO. The appearance of a small peak upon the O−H stretching vibration at 3300 cm^{-1} (NH_2 stretching vibration) and another peak at 810 cm^{-1} (N−H deformation vibration) indicates the presence of unreacted primary amine. The ammonolysis was confirmed by the changes in the peaks for the C═O stretching vibrations of the ester and amide groups. While the C═O stretching vibration of ester at 1736 cm^{-1} decreases with increasing molar ratio of DDA to ESO, the C═O stretching vibration of amide at 1646 cm^{-1} (amide I) and the N−H stretching vibration at 1551 cm^{-1} (amide II) increase. These changes indicate that the degree of ammonolysis increases with increasing molar ratio of DDA to ESO.

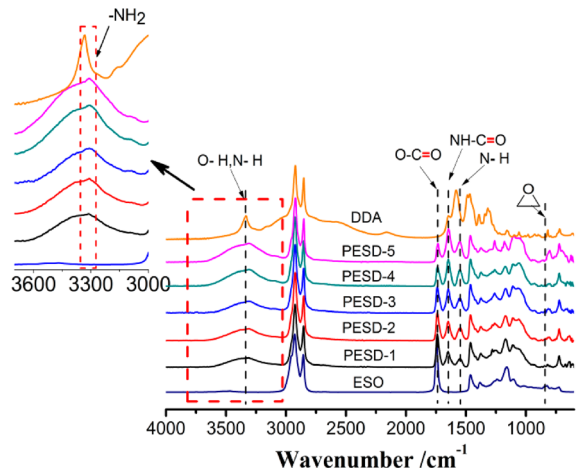

Figure 1. FTIR spectra of poly epoxidized soybean oil/decamethylene diamine (PESDs) and the reactants.

^{1}H NMR spectroscopy was used to identify the structures of PESD and determine the degree of ammonolysis. As shown in Figure 2a, the signals in the δ 2.90−3.10 ppm region, in the δ 4.00−4.41 ppm region, at δ 5.21 ppm, and at δ 3.20 ppm are

dx.doi.org/10.1021/ma301938a | Macromolecules 2012, 45, 9010−9019

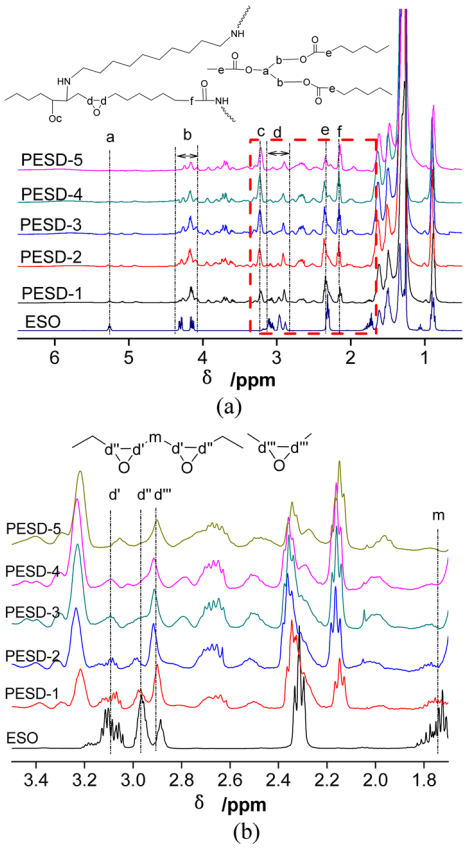

Figure 2. ^{1}H NMR spectra of ESO and PESDs: (a) full spectra and (b) magnification of region enclosed by rectangle.

attributed to the protons of epoxy group (d), the methylene protons of $-CH_2-CH-CH_2-$ (b), the methine proton of $-CH_2-CH-CH_2$ (a) and the proton of $-OH$ (c) respectively. It can be seen that with increasing molar ratio of DDA to ESO, (i) the signal coming from the epoxy group (d) weakens and the signal attributed to the resulting hydroxyl proton $-OH$ (c) increases, indicating that the reaction between amine and epoxy group occurred, and (ii) the signals coming from the methine proton of $-CH_2-CH-CH_2-$ (a), the methylene protons of $-CH_2-CH-CH_2-$ (b) and $-CH_2-COO-$ (e) weaken and the signal of the protons of $CH_2-CO-NH-$ (f) appears and increases, indicating that the ammonolysis indeed occurred. From the ^{1}H NMR data of PESD, as shown in Table 2, the degree of ammonolysis between the amine and the ester groups can be determined. When the molar ratio of DDA to ESO is below 2:1, only the peak area of the methine proton of $-CH_2-CH-CH_2-$ (a) decreases, while the peak area of methylene protons of $-CH_2-CH-CH_2-$ (b) remains unchanged, which indicate a low degree of ammonolysis. These results also indicate that the ester group adjacent to the methine has higher reactivity than the ester groups adjacent to methylene. With higher molar ratio of DDA to ESO, the peak area of the methylene protons of $-CH_2-CH-CH_2-$ (b) decreases, indicating an increase in the degree of ammonolysis. The higher reaction degree of ammonolysis finally resulted in lower molecular weight of the elastomer (see Table 1 and Scheme 1). In the spectrum for PESD-3, only the signal of the methine proton of $-CH_2-CH-CH_2-$ (a) disappeared while the signal of the methylene protons of $-CH_2-CH-CH_2-$ (b) remains the same. That is to say, just right one ester group of each glycerol center was broken. As a result, PESD-3 has the highest molecular weight. From the above analysis, we can see that, the amine is easier to react with epoxy group rather than ester group. Thus, the structure, molecular weight and gel content are all affected by the molar ratio of DDA to ESO.

According to the ESO structure, about 53.3% chains contain two adjacent epoxy groups. If the two epoxy groups in the same chain both react with DDA, a cross-linked structure will be formed. Since the PESD have low gel contents, it is reasonable to assume that only one of the two adjacent epoxy groups takes part in the ring-opening reaction. To verify this assumption, we analyzed the different protons of the epoxy groups. Figure 2b clearly shows the signals that come from the epoxy groups. The signal at δ 3.11 ppm, δ 2.95 ppm, δ 2.90 ppm, δ 1.73 ppm are attributed to —CH(O)—CH—CH$_2$—CH(O)—CH— (d′), —CH(O)—CH—CH$_2$—CH(O)—CH— (d″), —CH$_2$—CH(O)—CH—CH$_2$— (d‴) and —CH(O)—CH—CH$_2$—CH(O)—CH— (m), respectively. When the molar ratio of DDA to ESO is 2.5:1, the signal coming from —CH(O)—CH—CH$_2$—CH(O)—CH— (d′), —CH(O)—CH—CH$_2$—CH(O)—CH— (d″) and —CH(O)—CH—CH$_2$—CH(O)—CH— (m) almost disappear, while the signal attributed to —CH$_2$—CH(O)—CH—CH$_2$— (d‴) remains. The remaining epoxy group can be utilized in the cross-linking reaction. The phenomenon indicates that some epoxy groups did not react with diamine in spite of the increasing amount of DDA. The reason is that, when one of the two adjacent epoxy groups reacts with DDA, a large steric hindrance to the other epoxy group will be formed. The large steric hindrance of cause will prevent the other epoxy group from taking part in the reaction. The proposed reaction process is shown in Scheme 1. In order to focus on the major reaction between the amine and epoxy groups, we do not show the chain growth reaction in Scheme 1.

To better understand the process of the polymerization and the reactivity between amine and epoxy groups or ester groups, the products at different reaction times was studied by the ^{1}H NMR method. We have already shown that, the lower the molar ratio of DDA to ESO, the lower the degree of ammonolysis. Therefore, here PESD-3 and PESD-5 with high molar ratio of DDA to ESO were selected for study. The samples named PESD-3-*n*h and PESD-5-*n*h (n = 1, 2, 3, ...) were taken out of the reactor at 1 h intervals. The ^{1}H NMR spectra of PESD-3-*n*h and PESD-5-*n*h (as shown in the

Table 2. ^{1}H NMR Data of PESDs

	a	b	c	d	e	f
ESO	5.26 (1.0H)[a]	4.28, 4.15 (4.0H)	–	2.89–3.11 (8.0H)	2.36 (6.0H)	–
PESD-1	5.26 (0.4H)	4.28, 4.15 (4.0H)	3.23 (1.5H)	2.89–3.11 (3.0H)	2.36 (4.4H)	2.16 (1.6H)
PESD-2	5.26 (0.2H)	4.28, 4.15 (4.0H)	3.23 (2.0H)	2.89–3.11 (1.9H)	2.36 (4.2H)	2.16 (1.8H)
PESD-3	–	4.28, 4.15 (4.0H)	3.23 (3.0H)	2.89–3.11 (1.6H)	2.36 (4.0H)	2.16 (2.0H)
PESD-4	–	4.28, 4.15 (2.0H)	3.23 (3.8H)	2.89–3.11 (1.5H)	2.36 (2.0H)	2.16 (3.8H)
PESD-5	–	4.28, 4.15 (1.2H)	3.23 (4.2H)	2.89–3.11 (1.5H)	2.36 (1.2H)	2.16 (4.7H)

[a] 1.0H means there is 1.0H in one average construction unit according to the ratio of integral area with methyl proton as reference.

dx.doi.org/10.1021/ma301938a | *Macromolecules* 2012, 45, 9010–9019

Scheme 1. Schematic Diagram Showing Reaction Process with an Increasing Amount of DDA

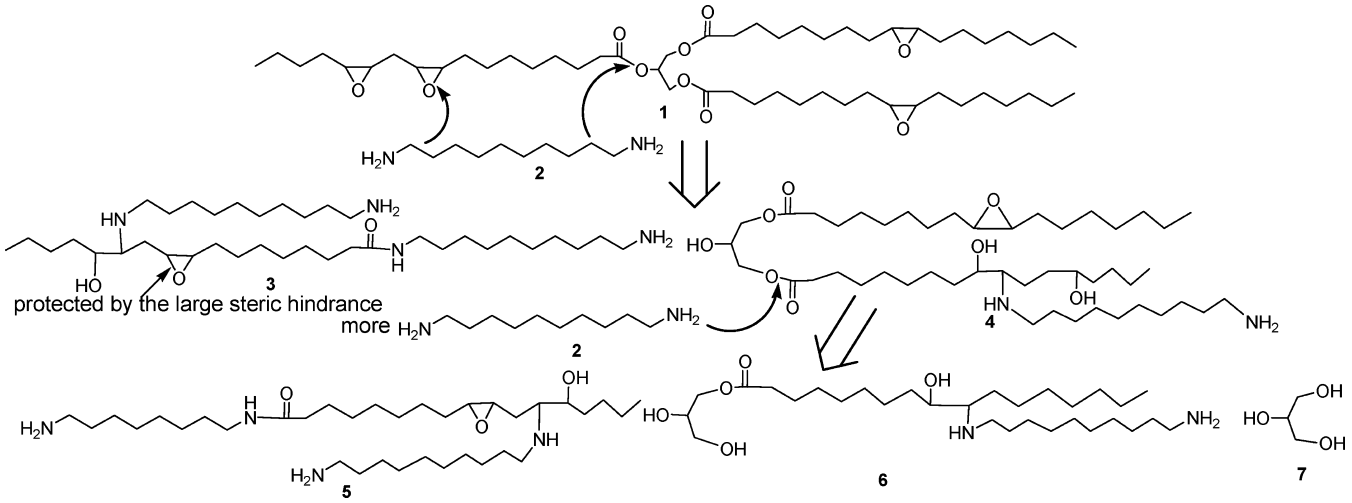

Supporting Information, Figure S2) showed the same trend. Therefore, we include the ^{1}H NMR results of only PESD-5-*n*h, as shown in Table 3, in our discussion. To our surprise, the peak area of the signals coming from the ester groups and epoxy groups simultaneously decreased significantly at the reaction time of 1 h. With increasing reaction time, the peak area of the signal attributed to the ester groups remains the same, while the peak area of the signal coming from the epoxy groups keeps decreasing. This phenomenon indicates that at the beginning of the reaction, an adequate amount of DDA monomer with high reactivity could react with both the ester groups and the epoxy groups. However, after one amine group of DDA had reacted, the other amine group of DDA with a low reactivity could only react with the epoxy groups slowly (Scheme 2). Then, the molecular weight continuously increased, and at last a polymer with adequate molecular weight climbed onto the stirrer shaft. The phenomenon also indicates that the epoxy groups (except the one that is protected by the large steric hindrance) have higher reactivity than the ester groups. By adjusting the molar ratio of DDA to ESO, different elastomer structures can be obtained as a result of the different degrees of ammonolysis. Thus, at a molar ratio of DDA to ESO of 2 to 1 (PESD-3), a linear polymer with many side chains and the highest molecular weight among the PESD was obtained as a result of both low degree of ammonolysis and high degree of reaction between epoxy and amine.

Table 3. ^{1}H NMR data of PESD-5 at Different Reaction Times[a]

	$-CH_2-C(-)H-CH_2-$	epoxy groups	$-CH_2-C(=O)-O-$	$-CH_2-C(=O)-NH-$
PESD-5-1h	3.0H	3.9H	3.0H	2.9H
PESD-5-2h	2.9H	2.6H	2.9H	3.0H
PESD-5-3h	3.0H	2.1H	3.0H	3.0H
PESD-5-4h	3.0H	1.9H	3.0H	3.0H
PESD-5-5h	3.1H	1.7H	3.1H	3.0H
PESD-5-6h	3.0H	1.6H	3.0H	3.0H
PESD-5-7h	3.0H	1.5H	3.0H	3.0H

[a]1.0H means there is 1.0H in one average construction unit according to the ratio of integral area with methyl proton as reference.

3.2. Thermogravimetric Analysis. In the TGA and DTG thermograms of PESDs (see Figure 3), two thermal degradation stages can be identified. The weight loss of first degradation stage from 200 to 420 °C can be attributed to the degradation of ester groups, and the weight loss of the second degradation stage from 420 to 480 °C corresponds to the decomposition of normal polyamide. The DTG curves show that with increasing molar ratio of DDA to ESO, the weight loss at the first degradation step decreases and the weight loss at the second degradation step increases, further confirming the transition of ester into amide during the reaction.

3.3. Determination of Glass Transition Temperature. The glass transition temperature (T_g) is a very important index to elastomer. The lower the T_g of an elastomer is, the higher the elasticity at room temperature is. The DSC thermograms of the various PESDs are shown in Figure 4. With increasing molar ratio of DDA to ESO, the two melting peaks of ESO disappear and obvious glass transition steps appear. PESD-1 and PESD-2, obtained at low molar ratios of DDA to ESO, show distinct melting peaks at about 0 and 8 °C, respectively. The melting peaks were contributed by the oligomers that were generated without adequate DDA in the stepwise polymerization. With enough DDA, such as in PESD-3, PESD-4, and PESD-5, only glass transitions can be seen in the DSC thermograms. Because of their low glass transition temperatures, the PESDs are rubbery at room temperature and are thus potential elastomers. Among the three PESDs showing no melting behavior, PESD-3 has the lowest T_g at about −17 °C and the highest molecular weight. Thus, PESD-3 was selected for further processing to prepare cross-linked elastomers.

3.4. Cross-Linking of PESD-3. Because of their high processability, PESDs have a wide range of potential applications. Since PESD contains −OH, $-NH_2$, and epoxy groups, it can be cross-linked by using diacids or anhydrides as cross-linkers. PESD-3 and different fractions of succinic anhydride (3 phr, 5 phr, 7 phr, 9 phr, or 11 phr, phr stands for one gram per a hundred gram of elastomer) were mechanically mixed, molded, and further cross-linked at 160 °C. The Mooney viscosity (Z100 °C 1 + 4) of PESD-3 was

dx.doi.org/10.1021/ma301938a | *Macromolecules* 2012, 45, 9010−9019

Scheme 2. Schematic Diagram Showing Reaction Process with Extending Time

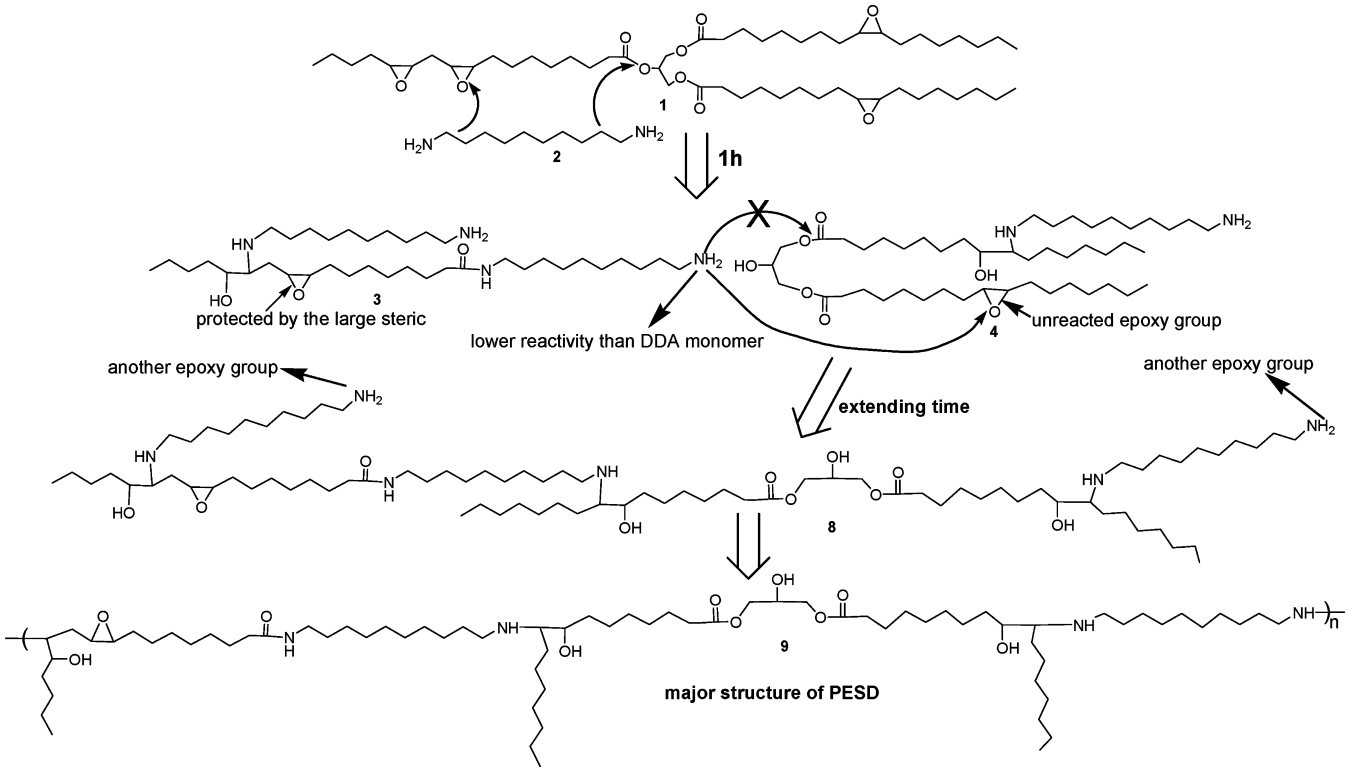

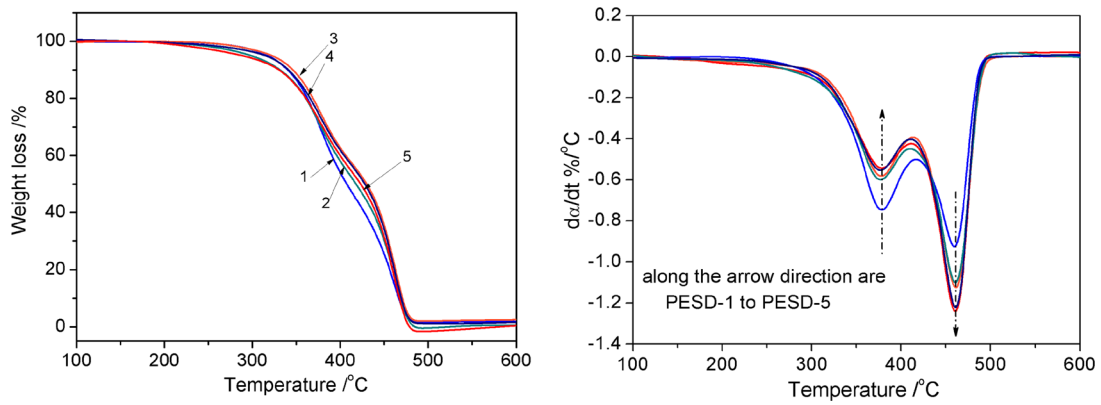

Figure 3. TGA and DTG curves of PESDs. 1−5 stand for PESD-1, PESD-2, PESD-3, PESD-4, and PESD-5, respectively.

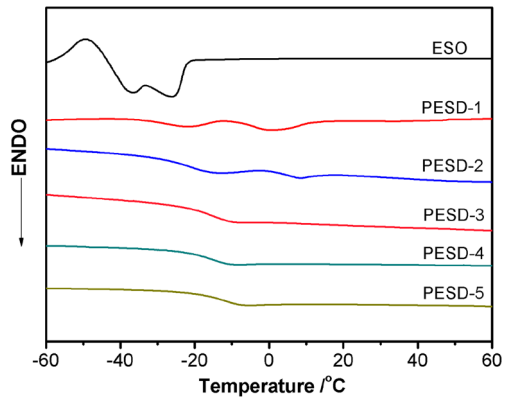

Figure 4. DSC curves of PESDs and ESO.

about 2.5 (see the Supporting Information, Figure S3). The low Mooney viscosity of PESD-3 leads to a good fluidity during shaping, so that PESD-3 has advantage in the preparation of some complex-shaped products or small/delicate products. In order to determine the cross-linking reaction mechanism, ^{13}C NMR was used to study the cross-linked bioelastomer. As shown in Figure 5, with increasing fraction of anhydride, the signals at δ 63 ppm and δ 70 ppm coming from the epoxy group and hydroxyl group slightly decreases while the signals at δ 171 ppm and δ 178 ppm attributed to the ester group and amide group increase. These changes indicate that the reaction between the anhydride and the amine group, epoxy group and hydroxyl group together resulted in a cross-linked structure. It is worthy to notice that the epoxy group, which does not react at 130 °C because of the large steric hindrance, can react with succinic anhydride at 180 °C. The cross-linking dynamics of PESD was studied by using a vulcameter, and the results are shown in Figure 6. The cross-linking dynamics of PESD was similar to those of traditional rubbers. With increasing fraction of succinic anhydride, the torque increases, indicating an

dx.doi.org/10.1021/ma301938a | *Macromolecules* 2012, 45, 9010−9019

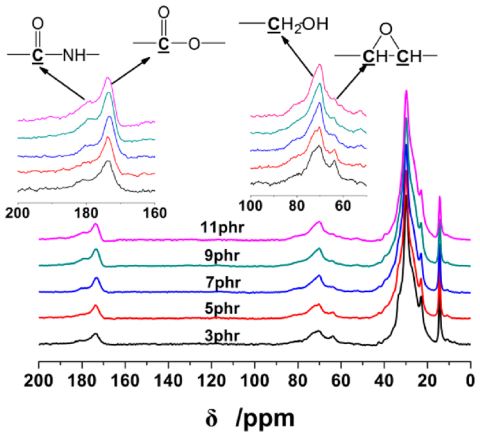

Figure 5. ^{13}C NMR spectra of cross-linked PESD-3 with different fractions of succinic anhydride.

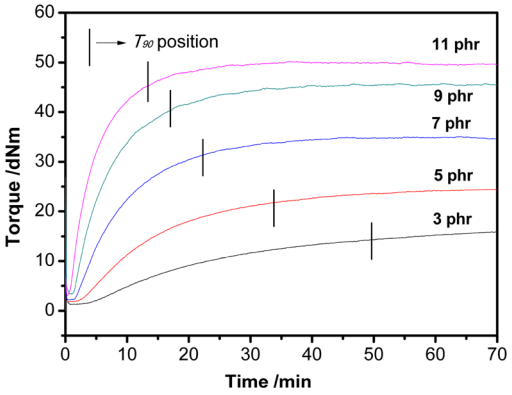

Figure 6. Cross-linking dynamic curves for PESD-3 with different fractions of succinic anhydride.

increase in cross-linking density. The T_{90} (the time when the torque reaches 90% of the maximum torque) data indicated that an increase in the fraction of cross-linker can accelerate the cross-linking process. The gel contents of PESD-3 produced by various quantity of cross-linkers range from 86% to 95%, as determined by a Soxhlet extraction method with tetrahydrofuran as the extractant. The glass transition temperature of the cross-linked bioelastomer was obtained by the DSC method. As shown in Figure 7, the glass transition temperature increases from −5 to +17 °C as the fraction of cross-linker increases. No

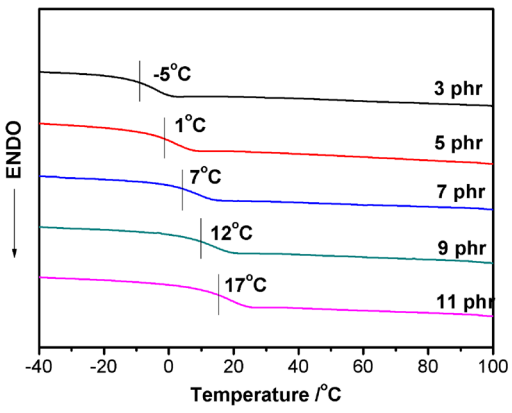

Figure 7. DSC curves for PESD-3 cross-linked with different fractions of succinic anhydride.

more than 11 phr of succinic anhydride should be used to obtain an elastomer at room temperature. The mechanical properties, damping property, water effects, and in vitro degradation of the bioelastomer was studied to explore the applicability of the soybean oil based bioelastomer.

3.5. Mechanical Properties. The typical elastic stress−strain curves of the bioelastomer without reinforcement by nanofillers are shown in Figure 8. The tensile modulus at a

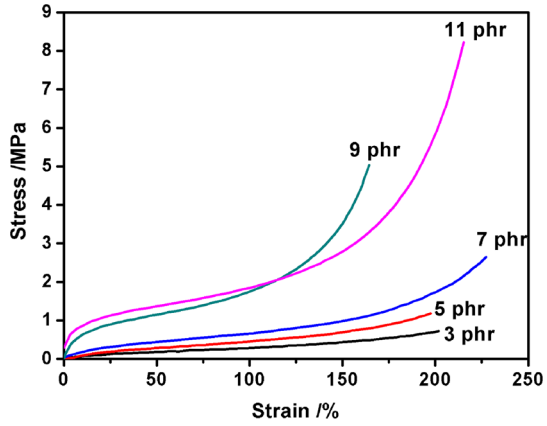

Figure 8. Stress−strain curves for PESD-3 cross-linked with different fractions of succinic anhydride.

given strain and the tensile strength of the bioelastomer generally increase with increasing succinic anhydride fraction. In the low strain region, the stresses are all low and slowly increase with increasing strain. When the strain is higher than about 110% and the succinic anhydride content is higher than 9 phr, the stress increases sharply because of the subsequent orientation of molecular chains. To the best of our knowledge, except for rubbers that crystallize under tensile stress (such as natural rubbers), most rubbers have tensile strengths ranging from 1 to 3 MPa and thus need to be reinforced by nanoparticles.[48] As to the soybean-oil-based bioelastomer, in the case of high cross-linker, the bioelastomer presents self-enhancement property which is mainly attributed by hydrogen bond and high T_g, while with low cross-linker, the bioelastomer would have to be reinforced with nanoparticles to have adequate tensile strength. The mechanical properties are listed in Table 4. The Shore A hardness and modulus at 100% elongation of the cross-linked bioelastomer are both tunable by varying the fraction of cross-linker.

3.6. Damping Property. DMTA testing was used to study the damping property of the bioelastomer. A high and broad tan δ peak is essential for good damping performance. Figure 9 shows the temperature dependence of the loss factor, tan δ, for the bioelastomer. For each bioelastomer, only one single broad tan δ peak is observed. With increasing fraction of succinic anhydride, the tan δ peak shifts to higher temperatures. These shifts indicate increasing glass transition temperature. It worth noting that, the temperature range (ΔT) for effective damping (tan δ higher than 0.3) is larger than 50 °C and the maximum peak value is higher than 1.4 at all fractions of succinic anhydride (see Table 5). Both properties indicate good damping performance of the bioelastomer, which should find potential applications as damping material. In addition, the working temperature range of the bioelastomer could be controlled by adjusting the fraction of cross-linker.

dx.doi.org/10.1021/ma301938a | Macromolecules 2012, 45, 9010−9019

Table 4. Mechanical properties of PESD-3 crosslinked with different fractions of succinic anhydride

sample	PESD-3−3phr	PESD-3−5phr	PESD-3−7phr	PESD-3−9phr	PESD-3−11phr
shore A hardness	28	34	38	45	50
tensile strength/MPa	0.8	1.0	2.5	4.8	8.5
modulus at 100% elongation/MPa	0.2	0.3	0.5	1.8	1.8
elongation at break /%	205	200	226	160	210
permanent deformation /%	16	8	8	4	4

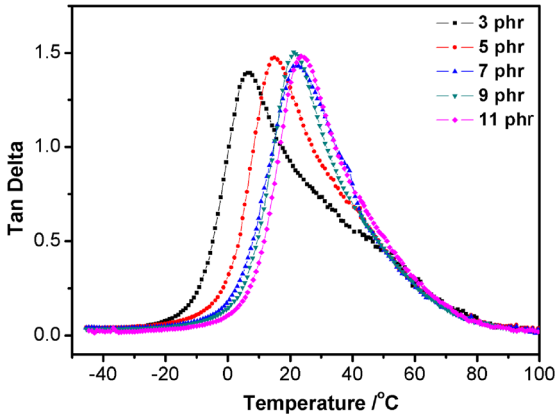

Figure 9. Temperature dependence of loss factor, tan δ, for PESD-3 cross-linked with different fractions of succinic anhydride.

Table 5. Glass Transition and Damping Properties of PESD-3 Cross-Linked with Different Fractions of Succinic Anhydride

sample	T_g[a] (°C)	T_g[b] (°C)	$(\tan\delta)_{max}$[c]	ΔT at tan $\delta > 0.3$[d] (°C)
3 phr	−5	6.6	1.40	66
5 phr	1	14.9	1.47	58
7 phr	7	21.1	1.43	54
9 phr	12	22.3	1.50	52
11 phr	17	23.8	1.48	52

[a]Glass transition temperature by DSC. [b]Glass transition temperature by DMTA. [c]Loss tangent (tan δ) maximum value. [d]The temperature range (ΔT) for efficient damping (tan $\delta > 0.3$).

3.7. Water Absorbance. The water absorbance of the bioelastomer was studied to explore potential engineering applications. The water absorbance of elastomers is theoretically affected by their polarity, and polar elastomers usually are hydrophilic. However, the polar bioelastomer we prepared are hydrophobic (water contact angle >90°), as shown by the water contact angle results in Table 6. The bioelastomer is hydrophobic because the fraction of amide groups is small and the hydroxyl groups are surrounded with aliphatic chains. In addition, −NH can form an intramolecular hydrogen bond with a hydroxyl to decrease its hydrophilicity. At the same time, the high content of ester groups can also decrease the hydrophilicity. The hydrophobic nature of the bioelastomer can also be seen from the water absorption data shown in Figure 10. With increasing time, the water absorption of the bioelastomer slightly increases and the water absorption values are all below 11 wt % after a soaking period of 576 h. The water absorption decreases with increasing amount of cross-linker. The absorption rate decreases with increasing time and approaches 0 at 576 h. According to the time of 10% water absorption, these bioelastomers have lower bibulous rates than most common rubbers.[49] The low bibulous rate makes these bioelastomers potentially applicable as engineering materials.

3.8. *In Vitro* Degradation Property. *In vitro* degradation of the bioelastomer was investigated by monitoring the change in weight loss during degradation in phosphate buffer solution (PBS). The weight loss of the bioelastomer quickly reaches a steady-state value in the first three days, as shown in Figure 11 because of some soluble substance. Afterward, the weight loss only slightly increases as a result of the slow degradation of the cross-linked structure and the high hydrophobicity of the bioelastomer. The low water degradation and low water absorption both indicate that the bioelastomer have potential applications as engineering rubbers.

4. CONCLUSIONS

By using a facile method, several soybean-oil-based and processable elastomers (PESDs) were successfully synthesized from ESO and DDA. There are three requirements for the formation of un-cross-linked elastomers: (i) the primary amine reacts with the epoxy groups, which will turn ESO into a polymer, (ii) the glycerol center of ESO is broken by ammonolysis, forming an un-cross-linked structure, and (iii) the generated −NH does not react with the epoxy group again and only one of the two adjacent epoxy groups in the same oil chain takes apart in the ring-opening reaction, which will avoid the formation of cross-linked structure. When one epoxy group reacts, the other one adjacent to it has a very low reactivity as a result of the large steric hindrance generated. On the basis of these requirements, several un-cross-linked elastomers with relatively low glass transition temperatures (−30 to −17 °C) were obtained in one-pot process by adjusting the molar ratio of DDA to ESO.

The reaction mechanism was determined by FTIR and ^{1}H NMR spectroscopy. When ESO reacts with DDA, (i) the ester group adjacent to the methine group has higher reactivity than the other two ester groups, (ii) epoxy groups (except the one that is protected by the large steric hindrance) has higher reactivity than the ester groups, (iii) both the epoxy groups and ester groups can react with DDA monomer, but only epoxy group can react with the other amine of DDA, one amine of which has already reacted.

The gel content and molecular weight of PESD are both affected by the molar ratio. The optimal molar ratio of DDA to ESO was found to be 2:1, which occurred in PESD-3, where just one ester group of each glycerol center reacts. With

Table 6. Water Contact Angle of PESD-3 Cross-Linked with Different Fractions of Succinic Anhydride

succinic anhydride content	3 phr	5 phr	7 phr	9 phr	11 phr
water contact angle (^{deg})	106.8 ± 0.3	107.3 ± 0.2	107.8 ± 0.3	108.2 ± 0.4	109.4 ± 0.2

dx.doi.org/10.1021/ma301938a | Macromolecules 2012, 45, 9010−9019

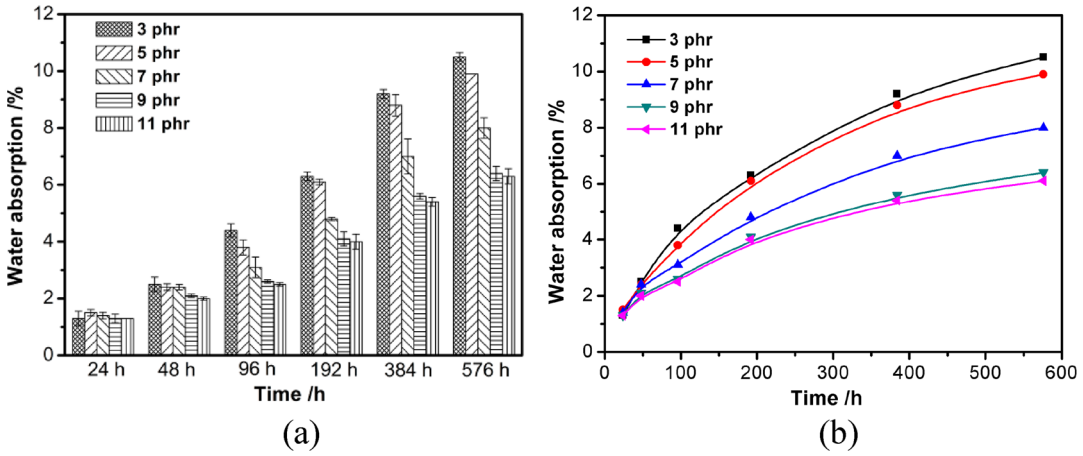

Figure 10. Water absorption of PESD-3 cross-linked with different fractions of succinic anhydride.

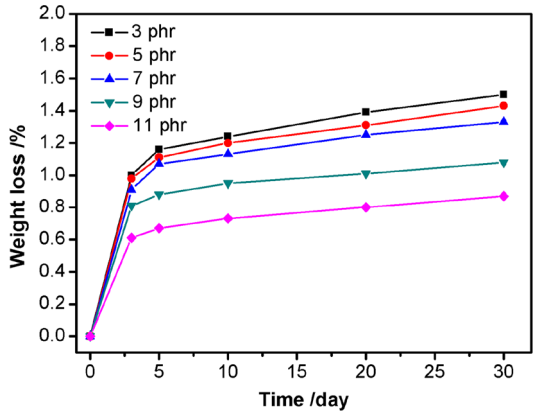

Figure 11. Degradation curves of PESD-3 cross-linked with different fractions of succinic anhydride.

increasing molar ratio of DDA to ESO, the number of ester groups broken by ammonolysis increases because the molecular weight decreases. Therefore, PESD-3 has the highest molecular weight and is suitable for further processing. Then, PESD-3 was processed according to normal rubber processing methods and cross-linked by succinic anhydride. The tensile strength of the bioelastomer with 11 phr succinic anhydride was 8.5 MPa and the elongation at break was about 200% without nanofiller reinforcement. DMA analysis revealed that the tan δ values of the bioelastomers are in the range of 1.4−1.5 and the damping temperature range are above 52 °C, suggesting that these bioelastomers show promise as damping materials. These bioelastomers also exhibited very low water absorption and PBS degradability. These novel bioelastomers prepared with non-petroleum dependent raw materials has practical values and can be used as the candidate of an engineering rubber.

■ ASSOCIATED CONTENT

Supporting Information

FTIR spectra of the product of ESO and dibutylamine at different reaction times, ^{1}H NMR spectra of (a) PESD-3-*n*h and (b) PESD-5-*n*h at different reaction times, and Mooney viscosity (Z100 °C 1 + 4) of PESD-3. This material is available free of charge via the Internet at http://pubs.acs.org.

■ AUTHOR INFORMATION

Corresponding Author

*Telephone: +86-10-6443-4860. Fax: +86-10-6443-3964. E-mail: Zhanglq@mail.buct.edu.cn.

Notes

The authors declare no competing financial interest.

■ ACKNOWLEDGMENTS

This work was supported by the National Natural Science Foundation of China (50933001), National Science Foundation for Distinguished Young Scholars (50725310), Project of Beijing Natural Science Foundation (2102020) and Science Fund for Creative Research Groups of the National Natural Science Foundation of China (51221002).

■ REFERENCES

(1) Bisio, A. L.; Xanthos, M. *How to manage plastics waste*; New York: Hanser Publishers: 1995.
(2) Mustafa, N. *Plastics Waste Management Disposal, Recycling and Reuse*; New York: Marcel Dekker: 1993.
(3) Meier, M. A. R.; Metzger, J. O.; Schubert, U. S. *Chem. Soc. Rev.* **2007**, *36*, 1788−1802.
(4) Eissen, M.; Metzger, J. O.; Schmidt, E.; Schneidewind, U. *Angew. Chem.* **2002**, *114*, 402−425.
(5) Sharma, V.; Kundu, P. P. *Prog. Polym. Sci.* **2006**, *31*, 983−1008.
(6) Sharma, V.; Kundu, P. P. *Prog. Polym. Sci.* **2008**, *33*, 1199−1215.
(7) Galià, M.; de Espinosa, L. M.; Ronda, J. C. *Eur. J. Lipid Sci. Technol.* **2009**, *111*, 1−9.
(8) Lu, Y. S.; Larock, R. C. *ChemSusChem.* **2009**, *2*, 136−147.
(9) Li, F.; Larock, R. C. *Biomacromolecules* **2003**, *4*, 1018−1025.
(10) Kundu, P. P.; Larock, R. C. *Biomacromolecules* **2005**, *6*, 797−806.
(11) Wang, H. J.; Rong, M. Z.; Zhang, M. Q.; Hu, J.; Chen, W. H.; Czigány, T. *Biomacromolecules* **2008**, *9*, 615−623.
(12) Hazer, B.; Hazer, D. B.; Çoban, B. *J. Polym. Res.* **2010**, *17*, 567−577.
(13) Çakmakli, B.; Hazer, B.; Tekin, İ. Ö.; Cömert, F. B. *Biomacromolecules* **2005**, *6* (3), 1750−1758.
(14) Hazer, D. B.; Hazer, B.; Kaymaz, F. *Biomed. Mater.* **2009**, *4*, 035011.
(15) Johnson, R. W.; Fritz, E. *Fatty acids in industry*; New York: Marcel Dekker; 1989.
(16) Heucher, R.; Butterbach, R. *Tappi J.* **1997**, *80* (6), 213.
(17) Li, F.; Hanson, M. V.; Larock, R. C. *Polymer* **2001**, *42*, 1567−1579.
(18) Valverde, M.; Andjelkovic, D.; Kundu, P. P.; Larock, R. C. *J. Appl. Polym. Sci.* **2008**, *107*, 423−430.

(19) Andjelkovic, D. D.; Larock, R. C. *Biomacromolecules* **2006**, *7*, 927−936.
(20) Andjelkovic, D. D.; Lu, Y. S.; Kessler, M. R.; Larock, R. C. *Macromol. Mater. Eng.* **2009**, *294*, 472−483.
(21) Wu, J. F.; Fernando, S.; Jagodzinski, K.; Weerasinghe, D.; Chen, Z. G. *Polym. Int.* **2011**, *60*, 571−577.
(22) Fu, L. Y.; Yang, L. T.; Dai, C. L.; Zhao, C. S.; Ma, L. J. *J. Appl. Polym. Sci.* **2010**, *117*, 2220−2225.
(23) Campanella, A.; Scala, J. J.; Wool, R. P. *J. Appl. Polym. Sci.* **2011**, *119*, 1000−1010.
(24) Bonnaillie, L. M.; Wool, R. P. *J. Appl. Polym. Sci.* **2007**, *105*, 1042−1052.
(25) Kim, H. M.; Kim, H. R.; Kim, B. S. *J. Polym. Environ.* **2010**, *18*, 291−297.
(26) Bunker, S. P.; Wool, R. P. *J. Polym. Sci., Part A: Polym. Chem.* **2002**, *40*, 451−458.
(27) Liu, Z. S.; Erhan, S. Z.; Xu, J.; Calvert, P. D. *J. Appl. Polym. Sci.* **2002**, *85*, 2100−2107.
(28) Liu, Z. S.; Doll, K. M.; Holser, R. A. *Green. Chem.* **2009**, *11*, 1774−1780.
(29) Lu, P. P. Doctoral dissertation, University of Missouri-Rolla: Rolla, MO, 2001.
(30) Rŏsch, J.; MüIhaupt, R. *Polym. Bull.* **1993**, *31*, 679−686.
(31) Pan, X.; Sengupta, P.; Webster, D. C. *Biomacromolecules* **2011**, *12*, 2416−2428.
(32) Javni, J.; Zhang, W.; Petrović, Z. S. *J. Appl. Polym. Sci.* **2003**, *88*, 2912−2916.
(33) Petrović, Z. S.; Zhang, W.; Javni, J. *Biomacromolecules* **2005**, *6*, 713−719.
(34) Keleş, E.; Hazer, B. *J. Polym. Environ.* **2009**, *17*, 153−158.
(35) Narine, S. S.; Kong, X. H.; Bouzidi, L.; Sporns, P. *J. Am. Oil. Chem. Soc.* **2007**, *84*, 55−63.
(36) Ivan, J.; Doo, P. H.; Petrović, Z. S. *J. Appl. Polym. Sci.* **2008**, *108*, 3867−3875.
(37) Wei, T.; Lei, L. J.; Kang, H. L.; Qiao, B.; Wang, Z.; Zhang, L. Q.; Coates, P.; Hua, K. C.; Kulig, J. *Adv. Eng. Mater.* **2012**, *14*, 112−118.
(38) Wang, R. G.; Ma, J.; Zhou, X. X.; Wang, Z.; Kang, H. L.; Zhang, L. Q.; Hua, K.; Kulig, J. *Macromolecules* **2012**, DOI: dx.doi.org/10.1021/ma301183k.
(39) Wang, Y.; Ameer, G. A.; Sheppard, B. J.; Langer, R. *Nat. Biotechnol.* **2002**, *20*, 602−606.
(40) Amsden, B.; Wang, S.; Wyss, U. *Biomacromolecules* **2004**, *5* (4), 1399−1404.
(41) Yang, J.; Webb, A. R.; Ameer, G. A. *Adv. Mater.* **2004**, *16* (6), 511−515.
(42) Nijst, C. L.; Bruggeman, J. P.; Karp, J. M.; Ferreira, L.; Zumbuehl, A.; Bettinger, C. J.; Langer, R. *Biomacromolecules* **2007**, *8* (10), 3067−3073.
(43) Bettinger, C. J.; Bruggeman, J. P.; Borenstein, J. T.; Langer, R. S. *Biomaterials* **2008**, *29* (15), 2315−2325.
(44) Ifkovits, J. L.; Padera, R. F.; Burdick, J. A. *Biomed. Mater.* **2008**, *3* (3), 034104.
(45) Yin, Y. China Patent, CN101088983, 2007.
(46) Bechthold, I.; Bretz, K.; Kabasci, S.; Kopitzky, R.; Springer, A. *Chem. Eng. Technol.* **2008**, *31* (5), 647−654.
(47) Corma, A.; Iborra, S.; Velty, A. *Chem. Rev.* **2007**, *107*, 2411−2502.
(48) Wang, Z. H.; Liu, J.; Wu, S. Z.; Wang, W. C.; Zhang, L. Q. *Phys. Chem. Chem. Phys.* **2010**, *12*, 3014−3030.
(49) Tang, B.; Li, X. Q.; Wang, J. W. *Ethylene-propylene rubber application technology*; Chemical Industry Press: Beijing, 2005.